

Comparison of ICESat Data With Airborne Laser Altimeter Measurements Over Arctic Sea Ice

Nathan T. Kurtz, Thorsten Markus, *Member, IEEE*, Donald J. Cavalieri, *Member, IEEE*, William Krabill, John G. Sonntag, and Jeffrey Miller

Abstract—Surface elevation and roughness measurements from NASA's Ice, Cloud, and land Elevation Satellite (ICESat) are compared with high-resolution airborne laser altimeter measurements over the Arctic sea ice north of Alaska, which were taken during the March 2006 EOS Aqua Advanced Microwave Scanning Radiometer sea ice validation campaign. The comparison of the elevation measurements shows that they agree quite well with correlations of around 0.9 for individual shots and a bias of less than 2 cm. The differences are found to decrease quite rapidly when applying running means. The comparison of the roughness measurements show that there are significant differences between the two data sets, with ICESat generally having higher values. The roughness values are only moderately correlated on an individual-shot basis, but applying running means to the data significantly improves the correlations to as high as 0.9. For the conversion of the elevation measurements into snow-ice freeboard, ocean surface elevation estimates are made with the high-resolution laser altimeter data, as well as several methods using lower resolution ICESat data. Under optimum conditions, i.e., when leads that are larger than the ICESat footprint are present, the ICESat- and Airborne Topographic Mapper-derived freeboards are found to agree to within 2 cm. For other areas, ICESat tends to underestimate the freeboard by up to 9 cm.

Index Terms—Ice, Cloud, and land Elevation Satellite (ICESat), laser altimeter, remote sensing, sea ice.

I. INTRODUCTION

THE DECLINE in Arctic sea ice cover as observed by satellite has recently received wide attention [2], [22]. The areal extent of sea ice has been monitored with satellites for nearly three decades, but much less is known about sea ice thickness. Nevertheless, recent studies have shown a thinning of the Arctic sea ice cover [17], [19]. Although there is an increasing number of *in situ* observations, including mass

balance buoys [18] and data from submarines [19], large-scale coverage can only be achieved from satellite observations. The Geoscience Laser Altimeter System (GLAS) on the NASA Ice, Cloud, and land Elevation Satellite (ICESat) can monitor the third dimension of the Earth's sea ice cover, its elevation above sea level, with unprecedented accuracy [20]. The instrument design and the mission requirements were determined by the main objective, which is to monitor the elevation changes of the ice sheets; however, recent studies suggest that the precision of ICESat is sufficient to provide useful information on the thickness of sea ice as well [12], [13]. Sea ice thickness h_i can be inferred from two quantities, namely, the freeboard portion fb of the sea ice and the snow depth h_s , assuming hydrostatic equilibrium, i.e.,

$$h_i = \frac{\rho_s}{\rho_w - \rho_i} h_s + \frac{\rho_w}{\rho_w - \rho_i} \text{fb} \quad (1)$$

where ρ_s , ρ_i , and ρ_w are the densities of the snow, sea ice, and water, respectively. The elevation measured by ICESat is the sum of the snow depth and sea ice freeboard. Therefore, in the following, the term freeboard will refer to the elevation of the sea ice above sea level plus its snow cover. A major challenge to convert ICESat-derived elevation to sea ice freeboard or, rather, the snow-ice-combined freeboard is knowing the elevation of the ocean surface as a reference height. In this paper, we evaluate the accuracy of the ICESat elevation data and the conversion to snow-ice freeboard using high-resolution airborne laser altimeter data collected during the EOS Aqua Advanced Microwave Scanning Radiometer (AMSR-E) Arctic sea ice validation campaign in March 2006 [3]. The data set for this flight consists of both outbound and inbound (return) flights, with both flight lines attempting to follow the predicted ICESat orbit.

In addition to elevation, surface roughness can be derived from ICESat data. Surface roughness is important because of its effect on the heat and momentum exchange between the atmosphere and ice but may also be important for determining the snow depth on the ice because the rougher surface can more effectively trap wind-blown snow [24]. Rough snow surfaces can also be a source of error in the retrieval of snow depth from passive microwave data [23]. The retrieved snow depth can be combined with the ICESat freeboard data to provide an estimate of sea ice thickness. The very high resolution of the airborne laser data also allows us to evaluate the ICESat roughness product.

Manuscript received July 5, 2007; revised December 7, 2007.

N. T. Kurtz is with the Joint Center for Earth Systems Technology, University of Maryland Baltimore County, Baltimore, MD 21250 USA.

T. Markus and D. J. Cavalieri are with the Hydrospheric and Biospheric Sciences Laboratory, NASA Goddard Space Flight Center, Greenbelt, MD 20771 USA.

W. Krabill is with the NASA Goddard Space Flight Center Wallops Flight Facility, Wallops Island, VA 23337 USA.

J. G. Sonntag is with EG&G Technical Services, Inc., Gaithersburg, MD 20878 USA, and also with the NASA Goddard Space Flight Center Wallops Flight Facility, Wallops Island, VA 23337 USA.

J. Miller is with RS Information Systems, McLean, VA 22102 USA, and also with the NASA Goddard Space Flight Center, Greenbelt, MD 20771 USA.

Color versions of one or more of the figures in this paper are available online at <http://ieeexplore.ieee.org>.

Digital Object Identifier 10.1109/TGRS.2008.916639

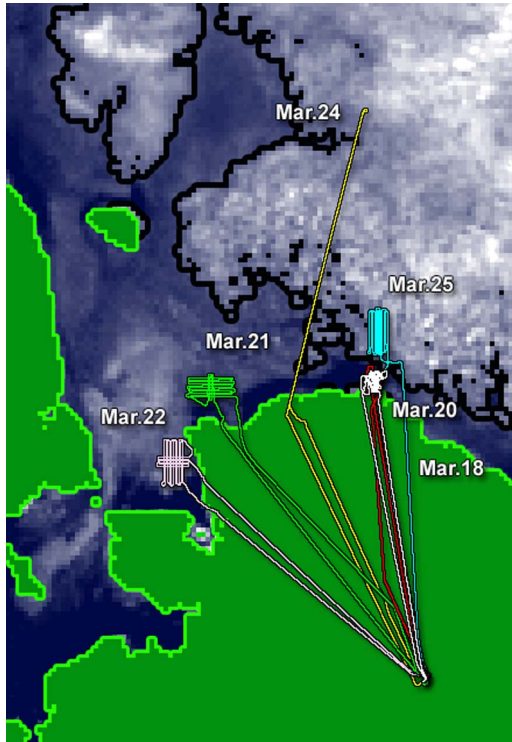


Fig. 1. Map of the AMSR-E Arctic sea ice validation campaign aircraft flights in March 2006 made from Fairbanks, AK. The flight on March 24 was coordinated with an ICESat overpass. The gray shades correspond to the AMSR-E snow-depth products. Areas outlined in black are multiyear ice for which no snow depth is retrieved. Shades in the multiyear-ice areas correspond to multiyear-ice concentration.

II. DATA

In March 2006, a coordinated Arctic sea ice validation field campaign using the NASA Wallops P-3B aircraft was successfully completed [3]. The purpose of this campaign was to validate the EOS Aqua AMSR-E sea ice products. Considering that ICESat was switched on during the period of the campaign, we coordinated one aircraft flight (on March 24, 2006) with an ICESat overpass (Fig. 1). During the period of the campaign, the Arctic weather was closely monitored to decide on a day when atmospheric conditions along the ICESat orbital track were expected to be mostly cloud-free. The mostly cloud-free conditions were also seen in the low gain (*i-gval-rcv* in the ICESat data product) for many of the shots in the transect, indicating a high signal-to-noise ratio. Various filtering methods have been suggested to select the data with more reliable elevation returns [13], but this was not found to be necessary for this paper due to the ideal atmospheric conditions. The end point of the aircraft return flight nearly coincided with the time of the ICESat overpass, and the total flight time over the sea ice was about 6 h. Thus, the time difference between the ICESat and aircraft measurements at the beginning of the outbound (northward) flight was about -6 h, -3 h at the turning point, and no time difference at the end of the inbound flight.

The flight line was determined by the predicted ICESat orbit. Fig. 2 shows the differences between the predicted ICESat orbit and the actual ground spot measurements, as well as

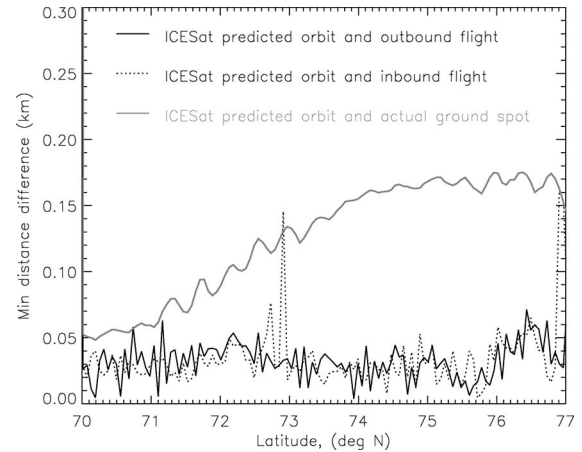


Fig. 2. Distances between predicted ICESat orbit, the actual ICESat ground spot measurements, and the aircraft flight lines. The aircraft attempted to follow the predicted orbit, and as the distance between the aircraft and ICESat ground spot measurement increased, the amount of overlap between the ICESat and ATM data decreased.

the differences between the predicted orbit and the outbound and inbound aircraft flights. While the distance between the predicted orbit and the airplane was expectedly small, the actual ICESat ground spot measurements drifted away from the predicted orbit with increasing latitude, with a maximum excursion of about 175 m at latitudes that are greater than 75° N. Errors in the horizontal geolocation of the ICESat data are expected to be on the order of several meters, although the actual geolocation errors for this laser campaign are unknown at this time. The horizontal geolocation errors in the aircraft laser altimeter data are expected to be much smaller at ≈ 0.5 m so that the error in overlap between the two measurements is expected to be small.

A. ICESat Data

ICESat measures the surface elevation relative to a reference ellipsoid using a 1064-nm laser. For the time period of this measurement, the footprint is an ellipse with a mean major axis of 52.3 m and eccentricity of 0.26, with measurements spaced at ≈ 170 -m intervals. Expected accuracy over low slope surfaces is approximately 14 cm for an individual measurement [27], with a precision of about 2 cm over smooth ice [13]. By analyzing the return waveform, properties such as average elevation, roughness, and reflectivity can be measured.

ICESat elevations are measured relative to the same ellipsoid as the TOPEX/Poseidon satellite. The ICESat data were converted to the WGS-84 ellipsoid for the purposes of this paper so that both data sets, ICESat and airborne laser altimeter data, have the same reference point. The ICESat elevation product is calculated by fitting a Gaussian function to the return waveform and taking the peak location of the Gaussian as the mean height of the surface. The geolocation and time of each measurement are then input into tidal models to correct for tidal effects so that the elevation is provided in a tide-free reference frame.

Surface roughness is given in terms of the standard deviation of the height in the footprint. By assuming a zero slope surface,

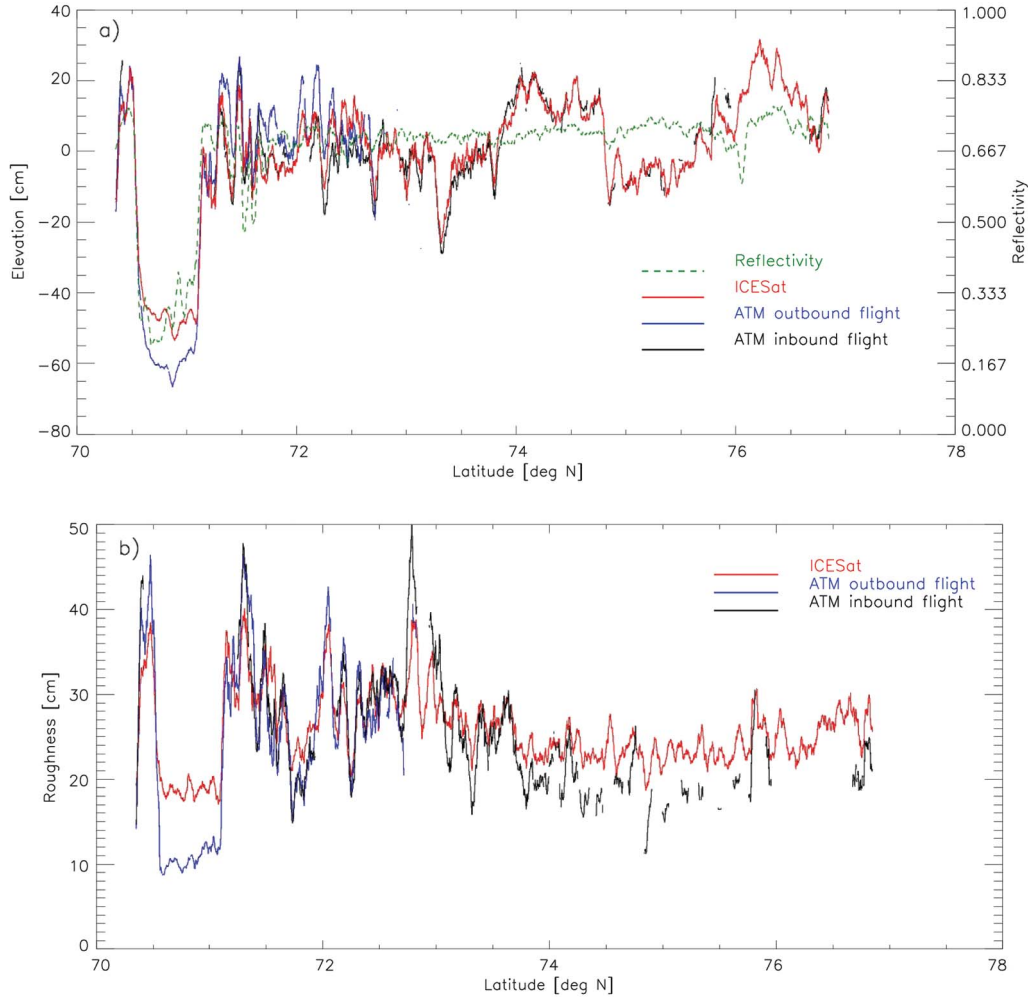


Fig. 3. Comparison between the 200-m ATM and ICESat data with no correction for ice motion. A running mean of 5.71 km was used to smooth the data. (a) Elevation comparison after the removal of the ArcGP geoid; both data sets are referenced to the WGS-84 ellipsoid and are corrected for tidal effects. Reflectivity, as measured by ICESat, is also plotted. (b) Roughness comparison.

which is appropriate for sea ice at the length scale of the footprint, the roughness can be calculated from the result of [5]

$$\sigma_{\text{surface}} = \frac{c}{2} (\sigma_s^2 - \sigma_f^2 - \sigma_h^2)^{\frac{1}{2}} \quad (2)$$

where σ_s^2 is the root-mean-square (rms) width of the Gaussian fit of the return waveform, σ_f is the rms transmitted pulsewidth assumed to be Gaussian in shape, and σ_h is the rms width of the GLAS detector impulse response. This result does not take into account the effects of atmospheric forward scattering which may broaden the return pulse possibly more so than that caused by the surface roughness, leading to overestimates in the calculated value.

B. Airborne Laser Data

Aircraft laser altimeter measurements were taken by the Airborne Topographic Mapper (ATM-4) [11], which is configured with a 15° off-nadir scanner. The ATM-4 is the latest version of a series of ATM instruments. Generally, the ATM is a conically scanning laser altimeter, which is combined with a differential GPS system for aircraft positioning and an

inertial navigation system (INS) to measure aircraft orientation. The combined laser range, GPS position, and INS orientation measurements are used to assign 3-D geographic coordinates to the point, where each laser pulse reflects from the surface. The system is calibrated by independent ranging measurements with the system on the ground and by overflights of presurveyed ground areas, which are usually airport ramps. The crossover comparisons of ATM results against surveys from other ATM flights and comparison with *in situ* results, including GPS surface transects, indicate that surface accuracy from the ATM is usually about 10 cm or better. The ATM data are referenced to the ITRF-2000 reference frame and projected onto the WGS-84 ellipsoid. The 15° scanner used during the mission yields a measured swath width of approximately half of the aircraft's altitude above the surface.

III. METHODOLOGY

To match the ATM data with the ICESat footprint, ATM elevation statistics within 55-m diameters of the ICESat locations are derived. For comparison with the 55-m footprint and to compensate for geolocation and ice motion errors, we also calculated statistics for 200-m diameters around the ICESat

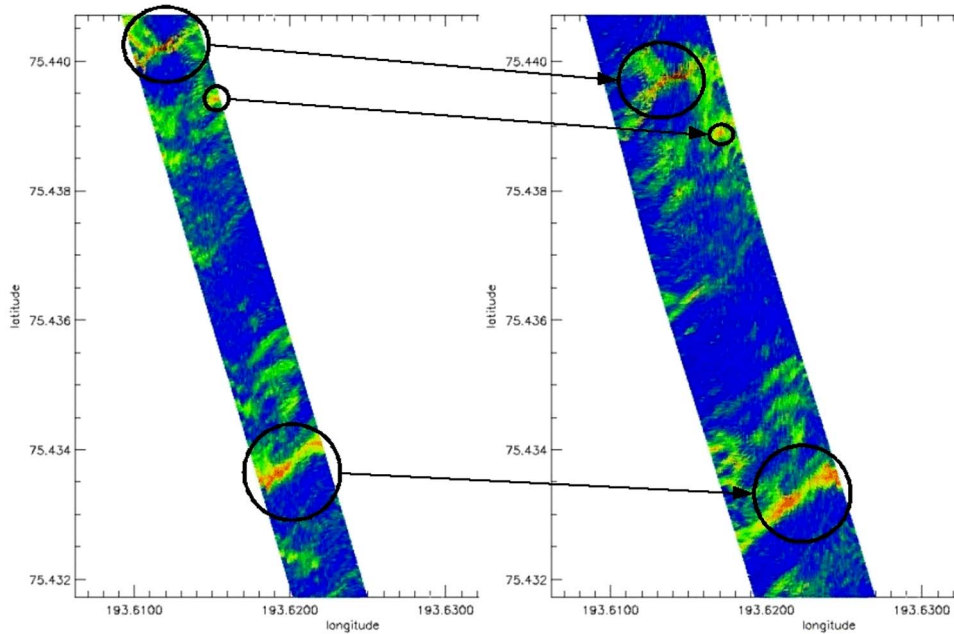


Fig. 4. Color representation of elevation profiles (blue are low elevation values and red are high elevation values) from the ATM inbound (right) and outbound (left) flights showing the movement of characteristic features. This movement was used to calculate the velocity of the ice for the region. Differences in the resolution and swath width of the ATM are due to the different altitudes of the inbound and outbound flights.

footprint center. The aircraft height above the ellipsoid was about 200 m on the outbound flight and 340 m on the inbound flight. That gives ATM swaths of 100 m (outbound) and 170 m (inbound) or 50 and 85 m to each side of the aircraft's centerline, respectively, and are an indication of the amount of overlap that is possible between the ATM and ICESat measurements with increasing distance between the two. The higher altitude of the inbound flight also leads to a lower number of total shots in the footprint area than the outbound flight. To maximize the accuracy and amount of data available for the flight, we required a minimum overlap of 50% of the total number of ATM points that are possible for the 55-m circles and 40% for the 200-m circles. For the 55-m-diameter circles this corresponds to approximately 300 and 600 points for the inbound and outbound flights, respectively, whereas for the 200-m-diameter circles, this corresponds to approximately 2900 and 3500 points for the inbound and outbound flights, respectively.

Fig. 3 shows the 200-m circle ATM elevation and roughness data as well as the corresponding ICESat data. The average amount of overlap was 60% and 85% for the inbound and outbound data, respectively. The reflectivity from ICESat is also plotted, for reference, on the figure. This reflectivity has not been corrected for atmospheric effects, but because of the clear sky conditions, is not significantly different from the corrected value (*i-reflCor-atm* in the ICESat data product). The overall agreement between the ATM and ICESat measured elevations is good, but areas with significant differences can be seen even between the ATM inbound and outbound flight data. A large part of these differences was found to result from the motion of the ice that occurred during the time between measurements.

To account for the effects of ice motion on the measurements, we derived ice velocities for approximately 60 points along the flight path by tracking the location and time differences between distinct features in the inbound and outbound eleva-

tion data (see Fig. 4). We then interpolated between each ice velocity measurement to get the velocity estimates for the full flight path. After correcting for ice motion, we looked at the variability of both elevation and roughness on different spatial scales using running means at different lengths. We first assess the accuracy of the ATM data by comparing the ATM inbound and outbound flight data, where the results are shown in Table I. The rms differences and correlation coefficients r^2 for elevation and roughness are shown for each footprint diameter (55 and 200 m). The two left columns show the averaging length, which is both in terms of the number of ICESat pixels and in kilometers. There is good agreement between the measured elevations of the ATM even on a single-footprint basis with correlations of 0.96 and 0.99 for the 55 and 200 m diameters, respectively, and rms differences of 14.7 and 10.5 cm. On an individual-footprint basis, the roughness values of the ATM inbound and outbound flights are only moderately correlated (columns 5 and 9 in Table I), suggesting that the roughness measurement may be more sensitive than the elevation to errors in the ice motion estimates.

The velocity estimates and time differences between the airborne laser measurements and ICESat were used to adjust the viewing coordinates for the airborne laser data to negate the effects of the motion of the ice. There is a large gap between 70.5° and 72° N latitude, where no ice velocity measurements could be made. Because of the large size of the gap, the ice velocities in this section were not interpolated and, thus, not used in the comparison with the ICESat. After correcting for ice motion, the average amount of overlap for the ATM footprints was 72% for both the inbound and outbound 55-m data and 74% and 81% for the 200-m inbound and outbound flight data, respectively. Figs. 5 and 6 show the ATM elevation and roughness data after a correction for the effects of ice motion has been applied. Comparison with Fig. 3 shows that

TABLE I
 COMPARISON STATISTICS OF THE **ATM INBOUND** AND **OUTBOUND** ELEVATION AND ROUGHNESS DATA FOR DIFFERENT RUNNING-MEAN LENGTHS AND FOR 55- AND 200-m-DIAMETER CIRCLES CENTERED ON THE ICESAT FOOTPRINT. THE RUNNING-MEAN LENGTHS ARE IN TERMS OF THE NUMBER OF ICESAT PIXELS AND THE CORRESPONDING DISTANCE, WHICH IS IN KILOMETERS, BETWEEN THEM. THE CORRELATION BETWEEN THE ATM INBOUND AND OUTBOUND ELEVATION AND ROUGHNESS DATA IS GIVEN IN THE r^2 COLUMN AND THE RMS DIFFERENCE IN THE RMS COLUMN. THERE WERE 2562 SAMPLES FOR THE 200-m CIRCLES AND 1804 SAMPLES FOR THE 55-m CIRCLES

Running mean		55 m				200 m			
length		Elevation		Roughness		Elevation		Roughness	
Pixels	Distance [km]	r^2	RMS [cm]						
1	-	0.96	14.7	0.56	8.7	0.99	10.5	0.81	5.0
3	0.52	0.98	11.0	0.73	5.1	0.99	10.0	0.89	3.4
9	1.56	0.99	9.5	0.86	3.0	0.99	9.1	0.94	2.1
15	2.60	0.99	9.1	0.9	2.4	0.99	8.9	0.96	1.7
21	3.63	0.99	9.0	0.92	2.2	0.99	8.8	0.97	1.6
27	4.67	0.99	8.9	0.93	2.0	0.99	8.7	0.97	1.5
33	5.71	0.99	8.8	0.94	1.8	0.99	8.7	0.98	1.4
39	6.75	0.99	8.8	0.94	1.8	0.99	9.1	0.97	1.4
45	7.79	0.99	8.8	0.94	1.8	0.99	9.1	0.98	1.4
51	8.82	0.99	8.8	0.94	1.8	0.99	9.0	0.98	1.3
57	9.86	0.99	8.8	0.94	1.7	0.99	8.5	0.98	1.3
63	10.90	0.99	8.8	0.94	1.7	0.99	8.5	0.98	1.3
69	11.94	0.99	8.8	0.95	1.6	0.99	8.4	0.98	1.3
75	12.97	0.99	8.8	0.95	1.6	0.99	8.4	0.98	1.3
81	14.01	0.99	8.8	0.96	1.5	0.99	8.4	0.98	1.3
87	15.05	0.99	8.8	0.96	1.5	0.99	8.4	0.98	1.3
93	16.09	0.99	8.8	0.96	1.5	1.0	8.3	0.98	1.3
99	17.12	0.99	8.8	0.96	1.4	1.0	8.3	0.98	1.3
105	18.16	0.99	8.7	0.97	1.4	1.0	8.3	0.98	1.2
111	19.20	0.99	8.7	0.97	1.4	1.0	8.3	0.99	1.2
117	20.24	0.99	8.7	0.97	1.3	1.0	8.2	0.99	1.2
123	21.28	0.99	8.7	0.97	1.3	0.99	8.6	0.98	1.2
129	22.31	0.99	8.6	0.97	1.3	0.99	8.6	0.98	1.2
135	23.35	0.99	9.1	0.97	1.3	0.99	8.6	0.98	1.2
141	24.39	0.99	9.1	0.97	1.3	0.99	8.5	0.98	1.2
147	25.43	0.99	9.1	0.97	1.3	0.99	8.5	0.98	1.2

ice motion effects can be a source of significant error in the comparison of the data sets even after averaging over many points. The ice velocity measurements show that there was very little movement of the ice before 70.5° N, which could explain the initial excellent agreement between the outbound flight data and the ICESat shown in Fig. 3.

The region between approximately 70.5° and 71.25° N in Fig. 3 is known, through aerial photography done during the outbound and inbound flights and as evidenced by the lower elevation of this region than the surrounding areas, to contain significant amounts of thin ice. This can further be seen in the low reflectivity of the area and is another demonstration that areas of low relative elevation and reflectivity in the ICESat data

are an indication of thin ice or open water, as shown by [12]. This thin ice area is also a cause for concern as there is a large, consistent elevation bias of more than 15 cm in some places between the outbound ATM data and ICESat. There are no direct ice motion measurements in this area due to the lack of inbound ATM data in this region; therefore, it is unknown how much of this difference is caused by ice motion effects. A coarse estimate of ice motion, through aerial photography, shows that the ice moved more than 200 m longitudinally in the time between the outbound and inbound flights so that the ice measured by the outbound flight and the ICESat were indeed different. However, the aerial photography of both the inbound and outbound flights, as well as the ICESat elevation

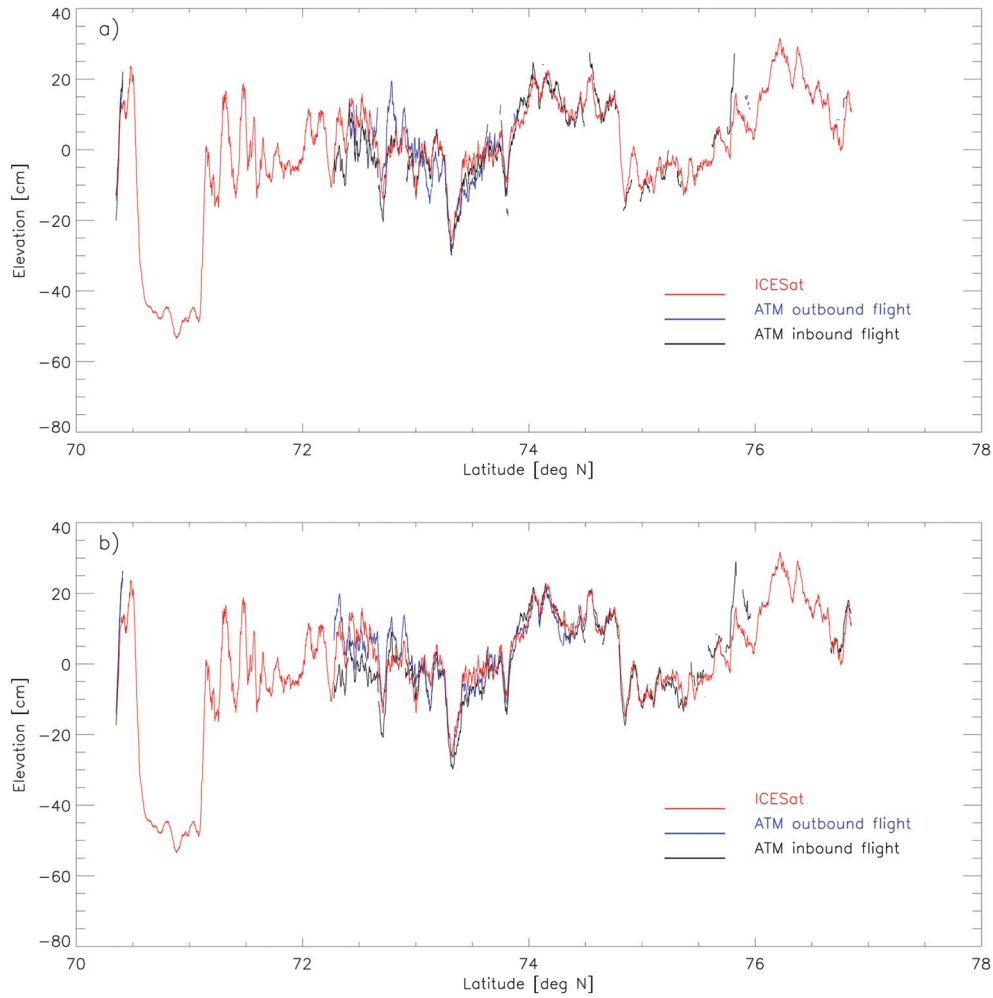


Fig. 5. Comparison between the ATM and ICESat elevation data after the removal of the ArcGP geoid and corrections for tidal effects and ice motion have been applied. Both data sets are referenced to the WGS-84 ellipsoid, and a running mean of 5.71 km was used to smooth the data. (a) ICESat elevation compared with the 55-m ATM data. (b) ICESat elevation compared with the 200-m ATM data.

and reflectivity data, all indicate that significant quantities of thin ice were being measured for all the data sets. Due to the low freeboard expected for thin ice, we do not expect such a large consistent bias in elevation to be caused by ice motion. The reason for this bias, and whether the bias is due to ICESat or the ATM, is not known.

IV. RESULTS

We first compare the elevation and roughness because they are directly inferable from the ICESat waveform before comparing freeboard estimates. The surface roughness can be defined in several different ways, but for consistency with the ICESat definition, we define the roughness from the ATM data as the standard deviation in elevation within the ICESat footprint.

A. Elevation and Roughness

Table II shows the comparison between the ice motion-corrected ATM and the ICESat data for both the elevation and roughness on different spatial scales. The rms differences and correlation coefficients r^2 for the elevation and roughness are

shown for both the inbound and outbound legs of the flight and for each footprint diameter (55 and 200 m). The correlation coefficients are above 0.9 for individual shots and increase quickly to 1.0 with increasing running-mean lengths. Similarly, the rms differences decrease to values of about 3 to 5 cm. The generally good agreement in the elevation data is also seen in Fig. 5. The 200-m-footprint data shown in Fig. 5 compare slightly better than the 55-m-footprint data despite being larger than the actual ICESat footprint. The correlation between ICESat and ATM data is high for any running-mean length and very close to 1.00 (columns 3 and 7 in Table II). As expected, the rms difference is decreasing with increasing averaging length. The average difference between the ATM and the ICESat elevations suggests a small or negligible bias for ICESat of 0.0 and -1.6 cm for the inbound and outbound 55-m data, respectively, and -0.6 and -0.8 cm for the inbound and outbound 200-m data, respectively, which is well within the expected range of 2 cm found by [16]. For comparison, the inbound flight elevations were an average of 3.6 cm higher than the outbound flight for the 55-m data and 2.1 cm higher for the 200-m data.

On an individual-footprint basis, ICESat and ATM roughness values are not well correlated, but the correlation

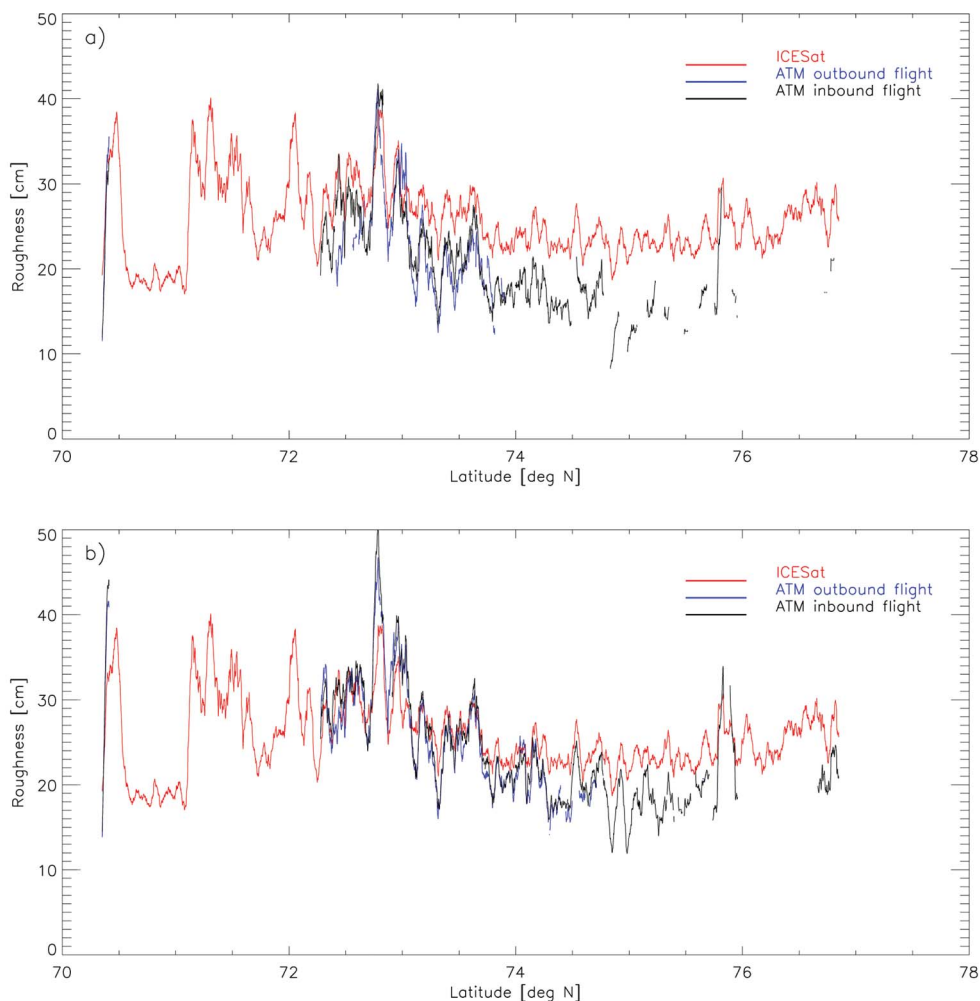


Fig. 6. Comparison of roughness between the ATM and ICESat data after a correction for ice motion has been applied. Roughness is defined as the standard deviation of the height in the footprint. A running mean of 5.71 km was used to smooth the data. (a) ICESat roughness compared with the 55-m ATM data. (b) ICESat roughness compared with the 200-m ATM data.

coefficients rapidly increase with the application of running means (columns 5 and 9 in Table II; Fig. 6). The correlation in roughness does not appear to depend on the ATM coverage within the ICESat footprint. The correlation with only those points most nearly representing the ICESat footprint (55-m-diameter circle around the ICESat footprint center with an overlap that is greater than 80%) was not any greater than the values reported in Table II. As mentioned earlier, forward scattering by the atmosphere is known to broaden the signal, which is possibly more so than that of the height distribution itself. A comparison with the ATM data shows that ICESat may tend to overestimate roughness; the average difference between the ATM roughness data and ICESat roughness is -5.9 cm (-6.3 cm) for the 55-m data and -2.0 cm (-2.7 cm) for the 200-m data. For comparison, the average difference between the ATM inbound and outbound roughness measurements is 0.8 cm for the 55-m data and 0.7 cm for the 200-m data. Between 74° and 75.5° N in Fig. 6, there appears to be signal broadening in the ICESat received waveform, which is not caused by variations in the height distribution because the roughness values correlate well in this region but appear to have a definite bias. The elevation in this region in Fig. 5 also

compares quite well, suggesting that the errors in roughness in this region are not caused by geolocation or overlap errors.

Detector saturation leads to a distortion of the received waveform and is known to cause a bias in the ICESat elevation. For moderately saturated returns, a correction to the elevation is given as a standard product (*i-satElevCorr*), whereas a related correction for the pulsewidth of saturated shots (*i-satPwDCorr*) for determining the roughness of surfaces with saturated return waveforms was not available. There were a total of 159 and 104 moderately saturated returns over the transect for the 55-m inbound and outbound data, respectively, and 164 and 168 for the 200-m inbound and outbound data, respectively; when these are removed, the correlations and rms differences do not noticeably improve. The rms differences and correlations for the single-shot saturated returns are nearly identical to the combination of saturated and unsaturated values for the entire transect shown in Table II. The only significant difference between the saturated and the single-shot values for the full transect was that the average saturated-shot elevation was about 4 cm lower than the corresponding ATM shot. This may not be very significant when one considers the relatively small number of points involved and that most of the points are in the region

TABLE II

COMPARISON STATISTICS OF ICE MOTION CORRECTED ATM AND ICESAT ELEVATIONS AND ROUGHNESS FOR DIFFERENT RUNNING-MEAN LENGTHS AND FOR 55- AND 200-m-DIAMETER CIRCLES CENTERED ON THE ICESAT FOOTPRINT. THE RUNNING-MEAN LENGTHS ARE IN TERMS OF THE NUMBER OF ICESAT PIXELS AND THE CORRESPONDING DISTANCE, WHICH IS IN KILOMETERS, BETWEEN THEM. CORRELATION BETWEEN THE ICESAT AND ATM ELEVATIONS AND ROUGHNESS IS GIVEN IN THE r^2 COLUMN AND THE RMS DIFFERENCE IN THE RMS COLUMN. RESULTS FOR THE OUTBOUND FLIGHT ARE IN PARENTHESES. THERE WERE 2637 (2641) SAMPLES FOR THE 200-m CIRCLES AND 2557 (1834) SAMPLES FOR THE 55-m CIRCLES

Running mean		55 m				200 m			
length		Elevation		Roughness		Elevation		Roughness	
Pixels	Distance [km]	r^2	RMS [cm]						
1	-	0.91(0.90)	20.9(19.6)	0.07(0.11)	14.1(13.5)	0.94(0.94)	17.0(16.0)	0.14(0.17)	11.2(11.1)
3	0.52	0.98(0.97)	9.6(10.5)	0.48(0.44)	8.6(9.0)	0.98(0.98)	9.9(9.2)	0.45(0.45)	7.2(7.2)
9	1.56	0.99(0.99)	5.9(6.7)	0.73(0.67)	6.9(7.4)	0.99(0.99)	6.9(6.0)	0.66(0.66)	5.2(5.3)
15	2.60	1.0(0.99)	5.2(5.8)	0.79(0.75)	6.6(7.1)	0.99(0.99)	6.2(5.1)	0.74(0.73)	4.6(4.8)
21	3.63	1.0(0.99)	4.9(5.4)	0.83(0.77)	6.4(6.9)	1.0(1.0)	5.9(4.6)	0.78(0.77)	4.3(4.5)
27	4.67	1.0(0.99)	4.8(5.1)	0.85(0.80)	6.3(6.9)	1.0(1.0)	5.7(4.3)	0.81(0.80)	4.2(4.3)
33	5.71	1.0(0.99)	4.7(4.9)	0.87(0.82)	6.3(6.8)	1.0(1.0)	5.6(4.2)	0.83(0.82)	4.0(4.2)
39	6.75	1.0(0.99)	4.6(6.2)	0.88(0.83)	6.2(6.8)	1.0(1.0)	5.5(4.0)	0.85(0.84)	3.9(4.1)
45	7.79	1.0(0.99)	4.5(6.2)	0.89(0.84)	6.2(6.8)	1.0(1.0)	5.4(3.9)	0.87(0.86)	3.8(4.0)
51	8.82	1.0(0.99)	4.4(6.2)	0.89(0.84)	6.2(6.8)	1.0(1.0)	5.3(3.8)	0.88(0.87)	3.8(3.9)
57	9.86	1.0(0.99)	4.4(6.2)	0.90(0.85)	6.2(6.7)	1.0(0.99)	5.2(4.9)	0.89(0.88)	3.7(3.9)
63	10.90	1.0(0.99)	4.3(4.8)	0.90(0.86)	6.2(6.7)	1.0(1.0)	5.1(3.6)	0.90(0.89)	3.7(3.8)
69	11.94	1.0(0.99)	4.3(6.1)	0.90(0.86)	6.2(6.7)	1.0(1.0)	5.1(3.5)	0.90(0.90)	3.7(3.8)
75	12.97	1.0(0.99)	4.2(6.1)	0.90(0.86)	6.2(6.7)	1.0(1.0)	5.0(3.5)	0.90(0.90)	3.7(3.8)
81	14.01	1.0(0.99)	4.2(6.2)	0.90(0.86)	6.2(6.7)	1.0(1.0)	5.0(3.4)	0.90(0.90)	3.7(3.8)
87	15.05	1.0(0.99)	4.2(6.2)	0.90(0.87)	6.1(6.7)	1.0(1.0)	5.0(3.4)	0.90(0.90)	3.7(3.7)
93	16.09	1.0(0.99)	4.2(6.2)	0.89(0.87)	6.1(6.7)	1.0(1.0)	4.9(3.3)	0.90(0.90)	3.6(3.7)
99	17.12	1.0(0.99)	4.1(6.2)	0.89(0.88)	6.1(6.7)	1.0(1.0)	4.9(3.3)	0.90(0.91)	3.6(3.7)
105	18.16	1.0(0.99)	4.1(6.1)	0.90(0.88)	6.1(6.7)	1.0(1.0)	4.9(3.2)	0.90(0.91)	3.6(3.7)
111	19.20	1.0(0.99)	4.1(6.0)	0.90(0.89)	6.1(6.7)	1.0(1.0)	4.9(3.2)	0.90(0.91)	3.6(3.7)
117	20.24	1.0(0.99)	4.1(6.0)	0.90(0.89)	6.1(6.6)	1.0(1.0)	4.8(3.1)	0.91(0.91)	3.5(3.7)
123	21.28	1.0(0.99)	4.1(6.0)	0.90(0.90)	6.1(6.6)	1.0(1.0)	4.8(3.1)	0.91(0.91)	3.5(3.7)
129	22.31	1.0(0.99)	4.1(6.0)	0.91(0.90)	6.1(6.6)	1.0(1.0)	4.8(3.0)	0.91(0.92)	3.5(3.6)
135	23.35	1.0(1.0)	4.1(4.3)	0.91(0.91)	6.1(6.6)	1.0(1.0)	4.8(3.0)	0.91(0.92)	3.4(3.6)
141	24.39	1.0(0.99)	4.0(4.3)	0.91(0.91)	6.1(6.6)	1.0(1.0)	4.8(2.9)	0.92(0.92)	3.4(3.6)
147	25.43	1.0(0.99)	4.0(4.3)	0.92(0.91)	6.0(6.7)	1.0(1.0)	4.8(2.9)	0.92(0.92)	3.4(3.6)

between 72.5° and 73.5° N where the elevation agreement is not as good.

B. Freeboard

Elevation and roughness can be directly inferred from the waveform, whereas the retrieval of the freeboard requires the additional knowledge of an ocean surface height as a reference.

The accurate derivation of sea ice freeboard is essential for determining a useful sea ice thickness, considering that even a small change in the freeboard leads to a large change in

the ice thickness. The sea-surface height (SSH) is a sum of many factors, including the geoid, dynamic topography, tides, and atmospheric pressure. The geoid is the largest contributor. The Arctic Gravity Project (ArcGP) [9] provides probably the best available geoid model for the Arctic. This geoid was first removed from all elevation data for freeboard estimation. The SSH cannot be modeled accurately enough at this time for the knowledge of elevation alone to be sufficient to calculate the freeboard. Therefore, several methods have been suggested for finding tie points to be used as the sea-surface reference height in a given area. It should be noted that the limited dynamic

TABLE III

COMPARISON OF THE AVERAGE FREEBOARD (IN CENTIMETERS) USING THE METHODS DESCRIBED IN SECTION IV-B FOR DETERMINING THE SSH. REGION 1 IS AN AREA CLOSE TO THE COAST LOCATED BETWEEN 70.45° AND 70.57° N, AND THE ATM DATA USED WERE THE 55-m FOOTPRINT OUTBOUND-FLIGHT DATA UNCORRECTED FOR ICE MOTION. REGIONS 2 AND 3 WERE LOCATED BETWEEN 75.2° AND 75.45° N AND 76.7° AND 76.8° N, RESPECTIVELY; THE ATM DATA USED WERE THE 200-m FOOTPRINT INBOUND FLIGHT DATA CORRECTED FOR ICE MOTION. THE NUMBERS IN PARENTHESES ARE FREEBOARDS AFTER REMOVAL OF THE 25 km RUNNING MEAN (FIRST NUMBER) AND 50 km RUNNING MEAN (SECOND NUMBER). THIS WAS DONE TO REDUCE UNCERTAINTIES IN THE GEOID AND TIDES, WHICH AFFECT BOTH DATA SETS

Sea Surface Height Method	Region 1	Region 2	Region 3
ATM freeboard	63.0 (60.6) (60.6)	36.8 (35.6) (35.6)	19.9 (21.8) (21.9)
Method 1: 50 km segments, no running mean removed	70.3	28.6	18.2
Method 2: 25 km segments, 25 km running mean removed	56.2	28.8	21.7
Method 3: 50 km segments, 50 km running mean removed	64.7	26.3	20.5

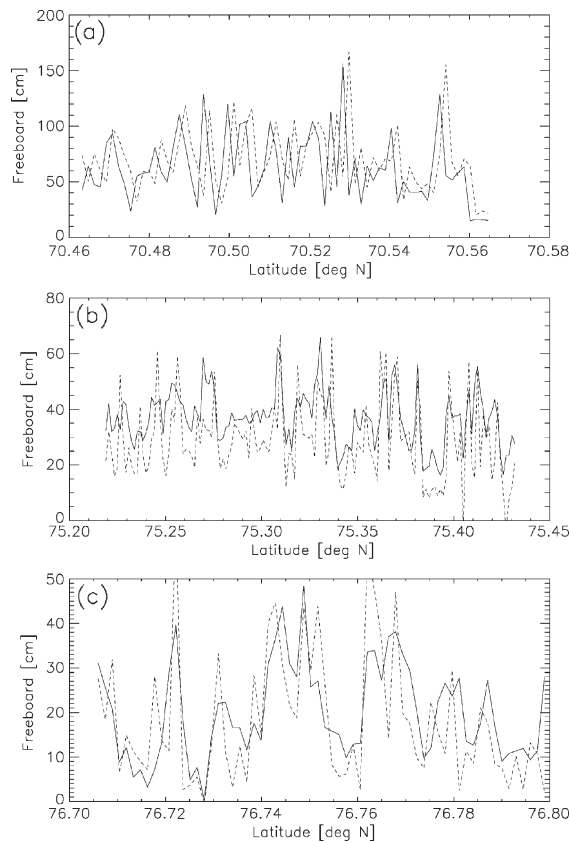


Fig. 7. Freeboard measurements for three regions where leads are known to exist (taken through aerial photography). The solid line is the ATM freeboard, whereas the dashed line is the ICESat-derived freeboard obtained by using the first method described in Section IV-B. (a) Region 1. This is a region close to the coast. The ATM data used for this region is the 55-m-footprint data uncorrected for ice motion. (b) Region 2. The ATM data used for this region is the 200-m-footprint data corrected for ice motion. (c) Region 3. The ATM data used for this region is the 200-m-footprint data corrected for ice motion.

range of the detector in the ICESat system causes the elevation measurements of very smooth specularly reflecting surfaces, such as ice or open water, to be unreliable. Lower reflectivity surfaces, such as thin-ice-filled leads or a rough sea surface, are needed to estimate the sea level.

We determine the SSH for the ATM data and then compare this with various methods of finding the SSH and freeboard using tie points from ICESat data only.

To obtain the SSH from the ATM data, areas of open water and newly refrozen leads of thin gray ice were first identified in aerial photographs which were taken coincident in time with

the ATM data. These areas were found to occur in groups, with nearly all the leads found near the beginning and end of the transect between 70.3° to 71.5° N and 75.5° to 77° N. The ATM elevation data were averaged to 7-m footprint sizes (containing a minimum of 50 individual ATM shots) in these areas, and the lowest was selected as the sea-surface reference height. This sea-surface reference height was used for all points within 12.5 km of the original measurement. The freeboard was then calculated by first removing the ArcGP geoid from the 55- and 200-m-footprint ATM data then subtracting the sea-surface reference height.

The following summarizes the different ICESat-only methods used to determine the SSH. Elevation refers to the elevation as measured by ICESat minus the ArcGP geoid for the point.

- 1) The ICESat transect is divided into separate 50-km regions. The lowest 1% (three values) of the elevations are averaged, and the resultant value is used as the sea level for each region.
- 2) The ICESat transect is divided into separate 25-km regions. It has been suggested that large-scale errors from the geoid and tidal models can be reduced by first subtracting a running mean of elevation from each elevation point and this may be a better starting point for the determination of the freeboard [14], [21]. A running-mean length of 25 km was removed from each point for this transect, and the average of the lowest two elevations in each 25-km region was used as the sea level.
- 3) The ICESat transect is divided into separate 50-km regions. A running-mean length of 50 km was first removed from each point, and the average of the lowest 1% (three values) of elevations in each 50-km region was used as the sea level.

Due to the fact that most of the areas with leads occurred where there were no overlapping ATM data, there is substantially less freeboard data than elevation data. There are three separate regions where the freeboard was computed by using each method along with the corresponding ATM freeboards given in Table III. The first region is in the latitude range of 70.45° to 70.57° N [Fig. 7(a)]. The ATM data used for this region were from the outbound flight, and the footprint size was 55 m. The data were not corrected for ice motion because no corresponding inbound flight data were available for this region. A clear and constant shift between the ATM and ICESat data can be seen due to the fact that no correction for the ice

motion was applied. This does not affect the results in Table III, where only the average freeboards are compared; however, one can see that a manual adjustment would bring the two data sets into excellent agreement. When using the first method, the average ICESat-derived freeboard for this area is within 7 cm of the ATM average freeboard, but a better agreement to within 4 cm is obtained after the removal of a large-scale running mean to reduce uncertainties from the geoid and tides.

Regions 2 and 3 were located between 75.2° and 75.45° N and 76.7° and 76.8° N, respectively [Fig. 7(b) and (c)], and the ATM data used were the 200-m-footprint inbound flight data corrected for ice motion. The 200-m data were used because there was an insufficient overlap with the 55-m data. Region 2 shows much less variability between the different ICESat methods used, but each method significantly underestimates the freeboard compared with the ATM-derived freeboard of 36.8 cm. The reason is most likely that the assumed open-water or thin-ice areas are contaminated by thick ice within the ICESat footprint. If a 55-m footprint from the ATM data is used as the reference sea level instead of the smaller 7-m footprint, then the average ATM freeboard becomes 27.5 cm, which is within 1 cm of the ICESat-derived freeboards. Thus, the contamination of ice within the footprint resulted in a bias of around 9 cm of the freeboard for this region. Region 3 shows a good agreement, considering that the ATM-derived freeboard is within 2 cm of all the ICESat-derived freeboards. The point with near-zero freeboard shown in Fig. 7(c) implies that nearly identical sea levels were correctly identified for both ICESat and the ATM.

The contamination of thick ice within assumed open-water or thin-ice regions in the ICESat footprint can create significant biases in the conversion of elevation to freeboard, as seen in region 2, whereas the points with no contamination lead to a good agreement with the freeboard, as seen in region 3. A more robust algorithm which only considers low elevations below a certain threshold as a sea-level tie point leads to a very small or insignificant bias but also to less data [14]. In a similar study but using a different method for finding the sea level, [4] obtained a freeboard bias of about 25 cm from the lowest level elevations of the ICESat measurements for a flight north of Greenland.

V. SUMMARY

ICESat elevation and roughness data were compared with ATM measurements over Arctic sea ice. Methods for converting ICESat elevation data into freeboard were also evaluated and compared with higher resolution ATM-derived freeboards.

The ATM data provide both an accurate and high-resolution measure of sea ice elevation. The similarities of the ATM and ICESat instruments make the ATM ideal for the direct comparison and validation of the satellite data. The ICESat and ATM data were compared for individual footprints and for different-length running means. ICESat sea ice elevations match very well with the ATM elevations with high correlation, even on an individual-footprint basis. With running-mean lengths of more than 1.6 km, the correlation is as high as 0.99. The rms difference between the two for the 200-m data is comparable to the previously reported uncertainty of ≈ 14 cm for a single ICESat

measurement. There is little, if any, elevation bias associated with this laser campaign. ATM roughness measurements show that the current ICESat roughness product tracks changes in roughness well, but that more work needs to be done to improve the retrieved accuracy.

The main goal of sea ice elevation measurements is the determination of sea ice thickness which requires freeboard measurements at the centimeter level. The elevation measurements of ICESat provide a first step toward this goal, but an accurate measure of sea-surface elevation is also required. Due to errors in the modeling of the sea-surface height, problems still exist in the conversion of elevation data into freeboard. Tie-point methods based on assumed open-water or thin-ice features are introduced to provide a more accurate sea-level estimate. Tie points, as measured by ICESat, can have a bias (9 cm for one region studied in this paper and 25 cm found in a separate study for an area that is north of Greenland [4]). The bias is a result of ice contamination within the footprint, which leads to an underestimation of the freeboard from the ICESat measurements alone. The actual bias for each region depends heavily on the sea state, ice concentration, and freeboard in the ICESat footprint. Ice contamination was not found to be a problem in region 3, and the average freeboard, as measured by ICESat and the ATM, were found to agree to within 2 cm, suggesting that a more selective algorithm for finding ICESat tie points than what was used here should provide good freeboard measurements where sufficient leads are present.

ACKNOWLEDGMENT

The authors would like to thank the mission manager and aircraft crew of the AMSR-E 2006 campaign for their contributions, and the reviewers for their constructive comments.

REFERENCES

- [1] A. C. Brenner, C. R. Bentley, B. M. Csatho, D. J. Harding, M. A. Hofton, J. Minster, L. Roberts, J. L. Saba, R. Schutz, R. H. Thomas, D. Yi, and H. J. Zwally, *Derivation of Range and Range Distributions From Laser Pulse Waveform Analysis for Surface Elevations, Roughness, Slope, and Vegetation Heights. Algorithm Theoretical Basis Document*. Greenbelt, MD: Goddard Space Flight Center, 2003. Version 3.0.
- [2] D. J. Cavalieri, C. L. Parkinson, and K. Y. Vinnikov, "30-year satellite record reveals contrasting Arctic and Antarctic decadal sea ice variability," *Geophys. Res. Lett.*, vol. 30, no. 18, pp. CRY4.1–CRY4.4, Sep. 2003. DOI:10.1029/2003GL018031.
- [3] D. J. Cavalieri and T. Markus, "EOS Aqua AMSR-E Arctic sea-ice validation program: Arctic 2006 aircraft campaign flight report," Goddard Space Flight Center, Greenbelt, MD, NASA/TM-2006-214142, 2006.
- [4] R. Forsberg and H. Skourup, "Arctic ocean gravity, geoid and sea-ice freeboard heights from ICESat and GRACE," *Geophys. Res. Lett.*, vol. 32, no. 21, p. L21 502, Nov. 2005. DOI:10.1029/2005GL023711.
- [5] C. S. Gardner, "Target signatures for laser altimeters: An analysis," *Appl. Opt.*, vol. 21, no. 3, pp. 448–453, 1982.
- [6] S. M. Hvidegaard and R. Forsberg, "Sea-ice thickness from airborne laser altimetry over the Arctic Ocean north of Greenland," *Geophys. Res. Lett.*, vol. 29, no. 20, pp. 13.1–13.4, Oct. 2002. DOI:10.1029/2001GL014474.
- [7] *IERS Conventions 2003*. IERS Tech. Note 32.
- [8] F. C. Jackson, "The reflection of impulses from a nonlinear random sea," *J. Geophys. Res.*, vol. 84, no. C8, pp. 4939–4943, Aug. 1979.
- [9] S. Kenyon and R. Forsberg, "Arctic gravity project: A status, in gravity, geoid and geodynamics 2000," in *Proc. Int. Assoc. Geod. Symp.*, M. G. Sideris, Ed., 2001, vol. 123, pp. 391–395.
- [10] J. Kouba, *A Guide to Using International GPS Service (IGS) Products*. IGS Publications Apr 2002 02 May 2007. [Online]. Available: http://igsceb.jpl.nasa.gov/components/IGSProducts_user_v17.pdf

- [11] W. R. Krabill, R. H. Thomas, C. F. Martin, R. N. Swift, and E. B. Frederick, "Accuracy of airborne laser altimetry over the Greenland ice sheet," *Int. J. Remote Sens.*, vol. 16, no. 7, pp. 1211–1222, May 1995.
- [12] R. Kwok, H. J. Zwally, and D. Yi, "ICESat observations of Arctic sea ice: A first look," *Geophys. Res. Lett.*, vol. 31, no. 16, p. L16 401, Aug. 2004. DOI:10.1029/2004GL020309.
- [13] R. Kwok, G. F. Cunningham, H. J. Zwally, and D. Yi, "ICESat over Arctic sea ice: Interpretation of altimetric and reflectivity profiles," *J. Geophys. Res.*, vol. 111, no. C6, pp. C06 006.1–C06 006.20, Jun. 2006. DOI:10.1029/2005JC003175.
- [14] R. Kwok, G. F. Cunningham, H. J. Zwally, and D. Yi, "Ice Cloud and Land Elevation Satellite (ICESat) over Arctic sea ice: Retrieval of freeboard," *J. Geophys. Res.*, vol. 112, C12 013, Dec. 2007. DOI: 10.1029/2006JC003978.
- [15] T. Markus and D. J. Cavalieri, "Snow depth distribution over sea ice in the Southern Ocean from satellite passive microwave data," in *Antarctic Sea Ice Physical Processes, Interactions and Variability, Antarctic Research Series*, vol. 74, M. O. Jeffries, Ed. Washington, DC: AGU, 1998, pp. 19–40.
- [16] C. F. Martin, R. H. Thomas, W. B. Krabill, and S. S. Manizade, "ICESat range and mounting bias estimation over precisely-surveyed terrain," *Geophys. Res. Lett.*, vol. 32, no. 21, p. L21 S07, Oct. 2005. DOI:10.1029/2005GL023800.
- [17] R. W. Lindsay and J. Zhang, "The thinning of Arctic sea ice, 1988–2003: Have we passed a tipping point?" *J. Clim.*, vol. 18, no. 22, pp. 4879–4894, Nov. 2005.
- [18] J. A. Richter-Menge, D. K. Perovich, B. C. Elder, K. Claffey, I. Rigor, and M. Ortmeier, "Ice mass-balance buoys: A tool for measuring and attributing changes in the thickness of the Arctic sea-ice cover," *Ann. Glaciol.*, vol. 44, no. 1, pp. 205–210, Nov. 2006.
- [19] D. A. Rothrock, Y. Yu, and G. A. Maykut, "Thinning of the Arctic sea-ice cover," *Geophys. Res. Lett.*, vol. 26, no. 23, pp. 3469–3472, Dec. 1999.
- [20] B. E. Schutz, H. J. Zwally, C. A. Shuman, D. Hancock, and J. P. DiMarzio, "Overview of the ICESat mission," *Geophys. Res. Lett.*, vol. 32, no. 21, p. L21 S01, 2005. DOI:10.1029/2005GL024009.
- [21] G. Spreen, S. Kern, D. Stammer, R. Forsberg, and J. Haarpaintner, "Satellite-based estimates of sea-ice volume flux through Fram Strait," *Ann. Glaciol.*, vol. 44, no. 1, pp. 321–328, Nov. 2006.
- [22] J. C. Stroeve, M. C. Serreze, F. Fetterer, T. Arbetter, W. Meier, J. Maslanik, and K. Knowles, "Tracking the Arctic's shrinking ice cover: Another extreme September minimum in 2004," *Geophys. Res. Lett.*, vol. 32, no. 4, p. L04 501, Feb. 2005. DOI:10.1029/2004GL021810.
- [23] J. C. Stroeve, T. Markus, J. A. Maslanik, D. J. Cavalieri, A. J. Gasiewski, J. F. Heinrichs, J. Holmgren, D. K. Perovich, and M. Sturm, "Impact of surface roughness on AMSR-E sea ice products," *IEEE Trans. Geosci. Remote Sens.*, vol. 44, no. 11, pp. 3103–3117, Nov. 2006.
- [24] M. Sturm, J. A. Maslanik, D. Perovich, J. C. Stroeve, J. Richter-Menge, T. Markus, J. Holmgren, J. F. Heinrichs, and K. Tape, "Snow depth and ice thickness measurements from the Beaufort and Chukchi seas collected during the AMSR-Ice03 campaign," *IEEE Trans. Geosci. Remote Sens.*, vol. 44, no. 11, pp. 3009–3020, Nov. 2006.
- [25] B. M. Tsai and C. S. Gardner, "Remote sensing of sea state using laser altimeters," *Appl. Opt.*, vol. 21, no. 21, pp. 3932–3940, Nov. 1982.
- [26] S. G. Warren, I. G. Rigor, N. Untersteiner, V. F. Radionov, N. N. Bryazgin, Y. I. Aleksandrov, and R. Colony, "Snow depth on Arctic sea ice," *J. Clim.*, vol. 12, no. 6, pp. 1814–1829, Jun. 1999.
- [27] H. J. Zwally *et al.*, "ICESat's laser measurements of polar ice, atmosphere, ocean, and land," *J. Geodyn.*, vol. 34, no. 3, pp. 405–445, Oct. 2002.



Nathan T. Kurtz received the B.S. degree in physics from Iowa State University, Ames, in 2004 and the M.S. degree in atmospheric physics from the University of Maryland Baltimore County, Baltimore, in 2007, where he is currently working toward the Ph.D. degree in atmospheric physics.

His current research interests include microwave and laser remote sensing of sea ice and snow cover.

Mr. Kurtz is a member of the American Geophysical Union.



Thorsten Markus (M'05) received the M.S. and Ph.D. degrees in physics from the University of Bremen, Bremen, Germany, in 1992 and 1995, respectively.

He was a National Research Council Resident Research Associate with the Goddard Space Flight Center (GSFC) from 1995 to 1996 before joining the NASA–University of Maryland Baltimore County (UMBC) Joint Center for Earth Systems Technology, UMBC, Baltimore, where he worked until 2002.

He is currently the Head of the Cryospheric Sciences Branch in the Hydrospheric and Biospheric Sciences Laboratory, NASA GSFC, Greenbelt, MD. His research interests include satellite remote sensing, and the utilization of satellite data to study cryospheric, oceanic, and atmospheric processes.

Dr. Markus is member of the American Geophysical Union.



Donald J. Cavalieri, (M'05) received the B.S. degree in physics from the City College of New York, New York, in 1964, the M.A. degree in physics from Queens College, New York, in 1967, and the Ph.D. degree in meteorology and oceanography from New York University, New York, in 1974.

From 1974 to 1976, he was a National Research Council Postdoctoral Resident Research Associate with the National Oceanic and Atmospheric Administration's Environmental Data Service, Boulder, CO, where he continued his doctoral research on

stratospheric-ionospheric coupling. From 1976 to 1977, he was a Visiting Assistant Professor with the Department of Physics and Atmospheric Science, Drexel University, Philadelphia, PA, where he worked on stratospheric temperature retrievals from satellite infrared radiometers. In the fall of 1977, he was a Staff Scientist with Systems and Applied Sciences Corporation, Riverdale, MD, where he worked on sea ice retrieval algorithms, in preparation for the launch of Nimbus-7 SMMR. In 1979, he joined the Laboratory for Atmospheres, NASA Goddard Space Flight Center, Greenbelt, MD, where he is currently a Senior Research Scientist with the Cryospheric Sciences Branch, Hydrospheric and Biospheric Sciences Laboratory. His current research interests include polar ocean processes and microwave remote sensing of the cryosphere.

Dr. Cavalieri is a member of the American Geophysical Union and the American Meteorological Society.



William Krabill received the B.S. degree in mathematics from Salisbury University, Salisbury, MD, in 1968.

In 1968, he joined NASA Goddard Space Flight Center Wallops Flight Facility, Wallops Island, VA, as a Mathematician and Data Analyst for the Radar Systems Section. He is currently the Project Manager and Principal Investigator (PI) for airborne lidar topographic mapping and Global Positioning System applications with the Cryospheric Sciences Branch of the NASA Goddard Space Flight Center/Wallops

Flight Facility. By 2000, the project had collected more than 4 billion surface elevation measurements over extensive portions of the Greenland Ice Sheet, with 65 000 km of track line in 1998 and 1999 alone. He has been the PI and Team Leader since 1991 for each of these annual Arctic deployments, managing the project and directing the planning, execution, and subsequent data processing and analysis.

Mr. Krabill is a member of the American Geophysical Union.



John G. Sonntag received the B.S. degree in aerospace engineering from Texas A&M University, College Station, in 1991 and the M.S. degree in aerospace engineering from the University of Texas, Austin, in 1993.

Since 1993, he has been with EG&G Technical Services, Inc., Gaithersburg, MD. He is currently with the NASA Goddard Space Flight Center Wallops Flight Facility, Wallops Island, VA, where he was a member of the NASA's Airborne Topographic Mapper project team. He specializes in the application of precise GPS positioning technology to airborne remote sensing problems and in the applications of airborne lidar mapping to polar science.



Jeffrey Miller received the B.S. degree in physics from the University of Maryland, College Park, in 1994.

From 1998 to 2004, he supported the Landsat Project Science Office at Goddard Space Flight Center (GSFC). He is currently with RS Information Systems, McLean, VA, supporting algorithm development and calibration at the NASA GSFC, Greenbelt, MD. His research interests are in radiometry, new data products, and improving product quality.